Physica B 610 (2021) 412786

Contents lists available at ScienceDirect

Physica B: Physics of Condensed Matter

journal homepage: http://www.elsevier.com/locate/physb

Electrical properties of 3 MeV proton irradiated silicon Schottky diodes

D.A. Oeba, J.O. Bodunrin, S.J. Moloi *

Department of Physics, College of Science, Engineering and Technology, University of South Africa, Private Bag X6, Florida, 1710, South Africa

ARTICLE INFO

Keywords:
Silicon diode
Current
Capacitance
Proton irradiation
Resistivity
Radiation detectors

ABSTRACT

This work presents the effects of proton irradiations on the electrical properties of *n*-silicon-based Schottky diodes. A change in electrical properties of the diodes due to 3 MeV proton irradiation to the fluence of 10^{17} ion cm^{-2} was investigated by current-voltage *(I-V)* and capacitance-voltage *(C-V)* techniques. A drastic decrease in forward current by a factor of 10^3 indicates a reduction of free injected effective carrier density in the space charge region. This reduction in the density is observed by a decrease in rectification ratio after proton irradiation. The results in general indicate that proton induced defects are responsible for the recombination/compensation of charge carriers resulting in an increase in the resistivity of the material. An increase in the resistivity is confirmed by high series resistance and low doping density evaluated on the irradiated diode. A change in dominated diode conduction mechanism due to irradiation presented here is of technological importance. Furthermore, the results presented here would, certainly, contribute to an ongoing study on the induced damage by radiation in silicon.

1. Introduction

Degradation of silicon (Si) detector efficiency has been a subject of interest due to both technological and scientific importance of the devices. The detectors are used in medical diagnostic technologies to detect abnormalities [1] and in high energy physics experiments [2]. The degradation is caused by defects that are induced by incident energetic particles. Radiation induced defects result into levels in the energy gap of Si that are responsible for a change in electrical properties of the material-based devices. Though studies on radiation damage has been ongoing for long [3–5], properties of the induced defects have not been fully understood and explanation of their effects on charge distribution mechanisms in the material is lacking in the literature.

An increase in material resistivity due the incident energetic particles was reported [6,7] on Si- based devices irradiated by neutrons and protons. This increase was explained in terms of radiation induced defects that are responsible for reduction in the majority carrier density in the depletion region. The data presented in Refs. [8,9], on the other hand, indicated a decrease in the device series resistance due to gamma radiation. This decrease in the series resistance stipulates a decrease in material resistivity due to radiation.

The observed degradation of the diode charge collection efficiency after proton irradiation [4] is an indication of radiation having detrimental effects on the devices. Though, it is known to have these unfavourable effects, irradiation has been found promising to improve radiation-hardness of Si [10,11]. A study on the effects of radiation on properties of the devices, therefore, continues to be of interest. A sufficient and reliable information on radiation effects on devices would lead to the establishment of suitable methods to improve detector's efficiency for the current and future applications.

In this work, a change in electrical properties of the fabricated *n*-Si-based diode due to proton irradiation was explained in terms of *I-V* plots generated in different scales. The effects of radiation on the diode capacitance were also investigated in this work. Both *I-V* and *C-V* techniques complement each other, and they provide information on charge distribution mechanisms and the resistivity of the material. Furthermore, a change in diode parameters such as, ideality factor, Schottky barrier height, saturation current, series resistance and doping density, due to radiation is presented in this work. The results presented could provide guidance to the study on conduction mechanisms involved in irradiated Si detectors, hence, establishment of a radiation-resistant material with improved material-based detector efficiency.

2. Experimental details

Devices studied in this work are unirradiated and proton irradiated Schottky diodes fabricated on crystalline *n*-Si. The resistivity and thickness of the material was quoted by manufacturer as 1–20 Ω cm and

* Corresponding author.
E-mail address: moloisj@unisa.ac.za (S.J. Moloi).

https://doi.org/10.1016/j.physb.2020.412786
Received 25 September 2020; Received in revised form 15 December 2020; Accepted 22 December 2020
Available online 24 February 2021

of 275 ± 25.0 μm, respectively. Prior to device fabrication, Si pieces were cleaned using standard cleaning procedure; methanol, acetone, trichloroethane and de-ionized water to remove any handling grease and residue. An oxide layer was removed by dipping the pieces into 40% hydrofluoric (HF) solution. The pieces were then blow-dried using nitrogen gas before loading into a high-vacuum chamber for diode fabrication.

The Schottky contacts were formed by vacuum evaporation of 130 nm gold (Au) through a mask of 0.6 mm diameter holes. The deposition was carried at ~10^{-6} mbar at the rate of 1 Å/s. The ohmic contact, on the other hand, was achieved by evaporation and deposition of 100 nm aluminium onto the unpolished side of the substrate. The finished devices each consists of 12 Schottky diodes on a piece and with one common ohmic contact.

The fabricated Schottky diodes were characterized using *I-V* and *C-V* techniques in the dark and at room temperature. Meters for current and capacitance measurements have been made in-house. The meters use the same hardware and they focus on software to implement the functions. The probe station was connected to the meters which is read by LabVIEW program specifically coded for these measurements. The contact between the device under test and the probe was determined accurately by enlarging the device under microscope.

During the measurements, the sample under test was placed in the test fixture (sample holder) for the voltage sweep run. A metallic shield was used to cover the test fixture to isolate the measurement system form the outside electromagnetic fields and keeping the probe station at a dark environment. Prior to irradiation, the measurements were taken on all the fabricated diodes. The characteristics of the diodes were found to be very similar such that it was safe to assume that all the diodes were one device irradiated by 3 MeV proton to the same fluence of 10^{17} ion cm^{-2}. The diodes that were not irradiated were labelled unirradiated diodes and those that were irradiated with protons were labelled irradiated diodes.

The *I-V* data were taken over the range of −3 to 3 V to ensure that tunneling electrons overcome thermionic emission electrons [12]. At the voltages higher than ~0.7 V, the bias voltage has a lower contribution of the thermionic emission current [12]. At the voltages above ±3 V, the forward current saturates due to the series resistance [13] and the reverse current was found to be less dependent on the applied voltage. Throughout the experiments, the time between measurements was maintained for 1 s to allow the device to stabilize.

The *C-V* measurements were taken at the measurement frequency of 20 kHz. After several trial with different frequencies, we realized that at the frequencies higher 20 kHz the acquired data was unstable since the measured capacitance was very low, close to the capacitance limit (pF) for our system. It was believed that the frequency of 20 kHz is the lowest that could be adopted for our devices to minimise the effects of metal-semiconductor (*m-s*) interface on the measured capacitance. Thus, at the measurement frequency ≥20 kHz charges at the interface states cannot follow an a.c signal [14]. Based on this measurement set-up, it was then safe to assume that the measured capacitance was mainly due to the space charge region.

3. Results and discussions

3.1. Current-voltage measurements

Fig. 1 shows *I-V* characteristics of unirradiated and irradiated diodes in a semilogarithmic scale. The forward current for both diodes increases linearly at low voltage range and deviates from linearity showing the effects of series resistance, R_S, at high voltage range [15]. It can also be observed from the figure that the forward current for irradiated diode is lower than that of unirradiated diode by a factor of ~10^3 at 3 V. The reverse current, on the other hand, has decreased by a factor of 4 due to irradiation. A drastic decrease in the forward current indicates that the recombination rate of majority carrier is higher than that of minority

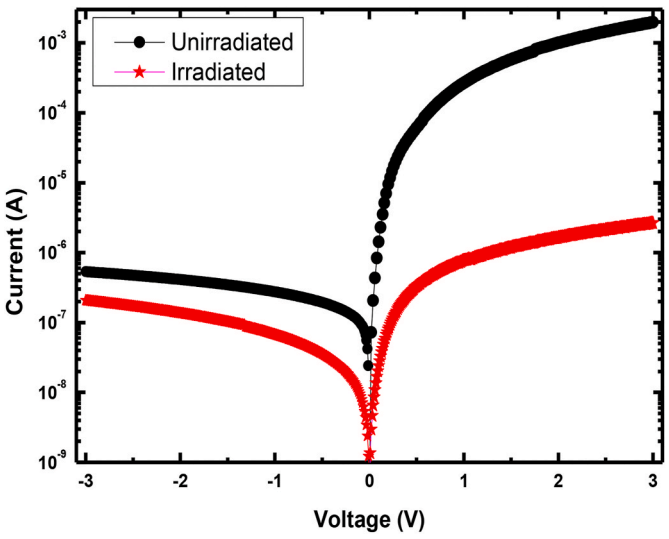

Fig. 1. I-V characteristics ofunirradiated and proton irradiated diodes in semi-logarithmic scale.

carriers resulting into a low charge carrier density through the space charge region after proton radiation.

A decrease in the current was reported before on the diodes irradiated with γ-particles [15,16]. In the case of the diodes fabricated on *p*-Si, a drastic decrease was observed in reverse current [15]. The results presented here agree with those presented before [8,15] to show that radiation induces defects that act as trapping or recombination centres to reduce the density of free charge carrier. These centres trap or recombine more electrons (majority/minority carriers in *n*-Si/*p*-Si) than holes. Reverse current trends for both diodes show non-saturation behaviour possibly due to the presence of a native interfacial layer between Au and Si [16–19].

Considering the effects of R_S, the current through the diode can be expressed in terms of thermionic emission theory [16] as

$$I = I_S \left[\exp\left(\frac{eV - IR_S}{\eta kT}\right)\right]. \quad (1)$$

The ideality factor, η, is calculated by substituting the slope of the linear region of the forward ln *I* - *V* plot as

$$\eta = \frac{e}{kT}\frac{dV}{d(\ln I)} \quad (2)$$

where $\frac{dV}{d(\ln I)}$ is the reciprocal of the slope of the linear region of the plot. η is a measure of the deviation from ideal diode behaviour. For the ideal diode, η is unity but in practice, it is always greater than 1. Factors that make the parameter to be greater than unity include the presence of an interface layer between the metal and Si, diode operation temperature and the generation or recombination of charge carriers in the material [20,21].

The saturation current, I_s , is derived from the straight linear fitting at zero bias and is expressed as

$$I_s = AA^*T^2\left(\frac{-e\Phi_B}{kT}\right) \quad (3)$$

where *A* is the diode area, A^* is the Richardson constant (=112 A-cm^{-2}-K^{-2}) for *n*-type Si, Φ_B is the Schottky barrier height given as

$$\Phi_B = \frac{kT}{e}\ln\left(\frac{AA^*T^2}{I_s}\right) \quad (4)$$

The flattening of the forward current curves at high voltages in Fig. 1 indicates that series resistance, R_S is an important parameter affecting electrical properties of the fabricated diodes [20].

Electrical parameters, η, I_s and Φ_B evaluated from unirradiated and irradiated diodes calculated using thermionic emission method are presented in Table 1. η evaluated for unirradiated diode is higher than unity confirming the existence of other charge distribution mechanisms, possibly a tunnelling mechanism. This tunnelling conduction mechanism could be due to the layer of SiO_2 formed between Au and Si resulting in a recombination of charge carriers through the interface states [21]. The same argument was provided based on the η of 1.12 and 1.17 evaluated on Au/*n*-Si diode with 1.5 and 2.5 nm metal-silicon interfacial layer thickness, respectively [22].

The value of η evaluated for irradiated diode is 2.72, higher than 1.67, evaluated on unirradiated diode. This increase in η indicates an involvement of generation-recombination charge distribution method in the material due to radiation induced generation-recombination (*g-r*) centres. G-*r* centres act as traps or recombination centres increasing the resistivity of the material. An increase in the resistivity is as a result of a decrease in the charge carrier density in the space charge region. This increase in material resistivity is confirmed by an increase in series resistance from 0.21 k Ω to 87.28 k Ω evaluated using d*V*/d(ln *I*)-*I* method and from 1.11 k Ω to 1130 k Ω using *H(I)-I* method [8,21].

The I_s evaluated for unirradiated diode is 46.40 nA which is higher than 13.7 nA reported in Au/ZnO thin film Schottky diodes fabricated on Si substrate [13] and lesser than 158 nA observed on Si PIN diode [12] indicating that the one obtained in this work is within an acceptable range. The value of I_s reduced after proton irradiation. The observed decrease in I_s was also observed on gamma-irradiated *p*-Si-based diode [15] and could be as a result of the trapping and recombination of carriers due to irradiation induced defects.

The Φ_B obtained in this study decreases after irradiation. It has been established that irradiation induces defects in the energy gap which affect free carrier concentration and lead to Φ_B decrease for *n*-type semiconductor [15]. Therefore, in this work, defects induced by proton irradiation reduced the carrier concentration in the depletion region through the occurrence of traps and recombination centres leading to an increase in Φ_B after irradiation.

Fig. 2 presents *I-V* characteristics of unirradiated (a) and proton irradiated (b) diodes in a logarithmic scale to study a change in diode conduction mechanisms due to proton irradiation. The trends for irradiated diode are lower than those of unirradiated diode indicating an increase in material resistivity after irradiation. The trends in Fig. 2 (b) are close to each other, especially at low voltages, showing a tendency of the diode exhibiting an ohmic *I-V* behaviour. Similar current trends were observed on the neutron irradiated [11] and on Au-doped n-Si -based diodes [23] and were explained in terms of *g-r* centres. The *g-r* centres are defect levels that are positioned at the centre of the energy gap of the material. The density of induced *g-r* centres at this radiation fluence is low making the trends not completely ohmic for the whole voltage range [11].

The rectification ratio, a ratio of the forward current to the reverse current at 3 V, for unirradiated diode is 1.02×10^4 and it is within the acceptable range in comparison to those obtained in the literature [12] indicating that the diodes were well fabricated. The ratio for irradiated diode, on the other hand, is evaluated to be 0.75×10^1. A decrease in rectification ratio is due to a decrease (increase) in the density of majority (minority) charge carriers [12]. This variation of the density implies that in *n*-Si, electrons are compensated or recombined with radiation-introduced acceptor levels to decrease the forward current or minority carriers (holes) are generated to increase the reverse current. The trends in Fig. 2, however, show that both currents have decreased with the forward current decreasing by the factor much higher than that of the reverse current after irradiation. This decrease in the current trends shows that the resistivity of the material has increased as charge carriers are compensated or recombined by radiation induced defect levels in the energy gap.

Table 1
The electrical parameters of unirradiated and proton irradiated *n*-Si diodes calculated using ln*I-V* method.

Diode	Parameters		
	η	Φ_B(eV)	I_s (nA)
Unirradiated	1.67	0.70	46.40
Irradiated	2.72	0.77	3.13

In Fig. 2 (a), a forward current trend shows three linear regions (i, ii and iii) with slopes of 1.85, 2.62 and 1.98, respectively. A slope of two or higher has been interpreted as indication of trapped charge-limited current (TCLC) with exponent trap distribution [16,24]. The charge distribution mechanism for this diode might be dominated by the space charge limited current (SCLC) with exponentially distributed surface states. According to the SCLC mechanism, when the applied voltage is increased, the injection of charge carriers from the electrode to the interface layer increases accordingly [16,24].

For the irradiated diode, slope of linear regions in Fig. 2 (b) were evaluated as 1.21, 1.68 and 1.14, respectively. Slopes close to unity for this diode indicates that the dominant conduction mechanism is ohmic. Ohmic behaviour is attributed to the domination of the generated current in the depletion region over the injected free carrier generated current [16,24]. The injected carrier density may be lower than the background thermal carrier density [24]. Thus, the density of the injected carrier from the material to the space charge region has decreased after irradiation. This reduction in the density is due to recombination/compensation of charge carriers by radiation-induced defect levels resulting in an increase in material resistivity. This increase in material resistivity is confirmed later in the text by a reduction in doping density due to irradiation.

3.2. Capacitance -voltage measurements

The capacitance, *C* of the fabricated diodes was measured as a function of voltage, *V*. The results presented in this study were derived from the depletion region capacitance in the reverse bias. In Schottky diodes, the junction capacitance is given [13] as

$$C = A\sqrt{\frac{e\varepsilon_s\varepsilon_0 N_D}{2(V_{bi}+V)}} \tag{8}$$

where ε_s is the dielectric constant of Si, ε_0 is the dielectric constant of free space, N_D is the doping density, V_{bi} is the built-in-voltage, and *V* is the applied voltage. From equation (8), it can be shown that the slope of the linear region of the C^{-2}- *V* plot can be used to determine the doping density while built-in-voltage can be determined using the intercept on the *V* -axis. For *n*-Si the built-in voltage is related to the Schottky barrier height [8] as

$$\Phi = V_{bi} + \frac{kT}{e}\ln\left(\frac{N_C}{N_D}\right) \tag{9}$$

where N_C is the effective density of state in the conduction band.

Fig. 3 (a) and (b) show *C-V* characteristics of unirradiated and proton irradiated *n*-Si-based diodes, respectively . The trends are similar with that of the irradiated diode being lower than unirradiated diode due to a decrease in free carrier density. This decrease in capacitance was also reported on the diodes irradiated with γ-particles [15]. Both trends show a gentle increase in capacitance at high voltage range. At low voltage range the capacitance increases exponentially as charge carriers are injected in the depletion region. The capacitance for unirradiated diode increases from ~0.024 nF at −3 V to ~0.061 nF at 0 V while that of the irradiated diode increases from ~0.008 nF to ~0.02 nF. A gentle increase in capacitance for irradiated diode indicates that the injection rate of free charge carrier in the depletion region has decreased. It should be noted that the full depletion width is not attained for these

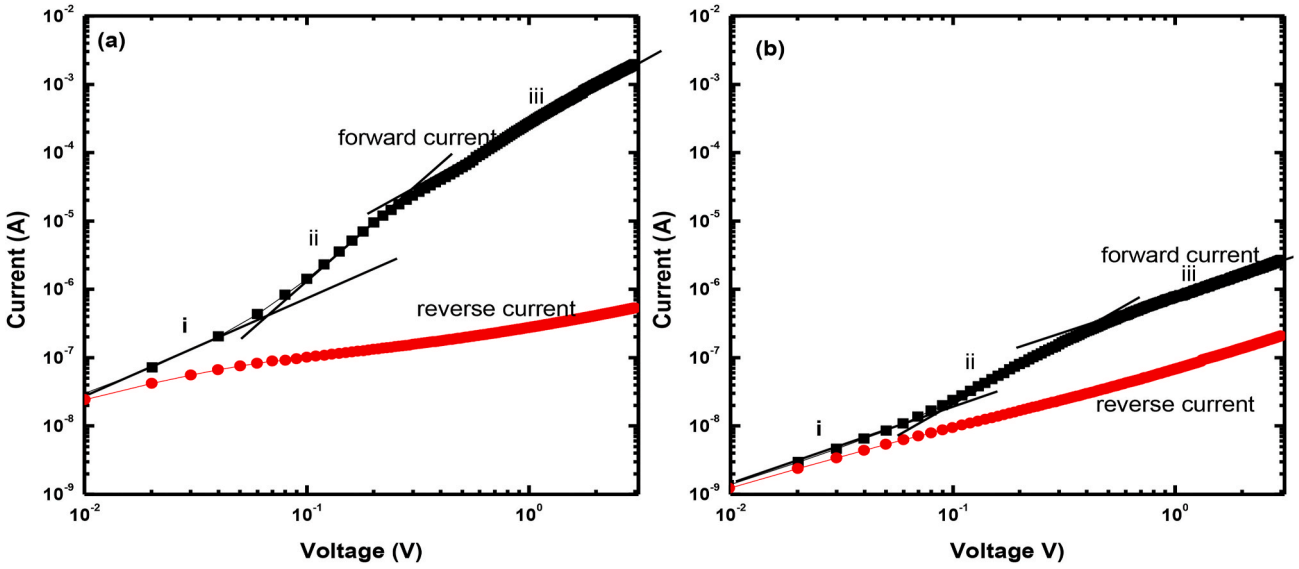

Fig. 2. The logarithmic I-V plots of unirradiated (a) and proton irradiated (b) diodes.

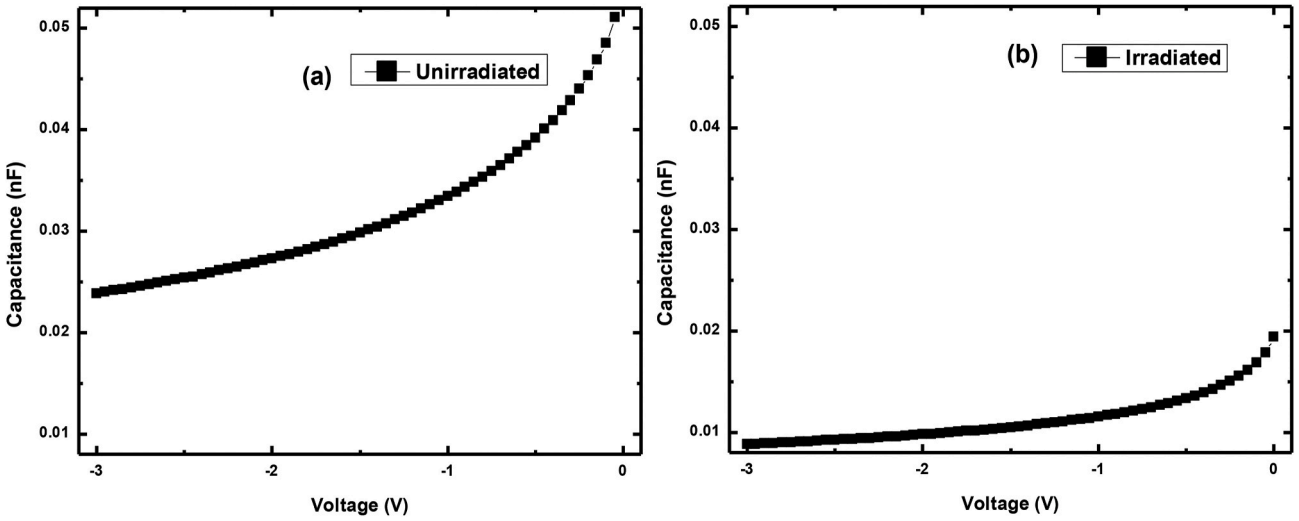

Fig. 3. C-V characteristics of unirradiated (a) and proton irradiated (b) diodes.

diodes since the measured capacitance does not show a tendency to saturate for both diodes.

Fig. 4 shows C^{-2}-V characteristics of unirradiated (a) and irradiated (b) diodes to study the doping profile of the devices. The plots were generated to determine the built-in voltage, doping density, and Schottky barrier height presented in Table 2. The plots shown in Fig. 4 are linear for the whole voltage range indicating a uniform doping density. The evaluated doping density for irradiated diode is 0.53 × 10^{15} cm^{-3} lower than 3.36 × 10^{15} cm^{-3} for unirradiated diode. A decrease in doping density is attributed to radiation-induced defects in the material. The defects are responsible for a decrease in mobile charge carrier density in the material by trapping them thereby decreasing the measured capacitance. Due to the trapping of mobile charge carriers, the resistivity of the material increases after irradiation. Using the relation, $\rho = (e\mu N_D)^{-1}$ the resistivity evaluated from unirradiated diode is 1.35 Ω cm and it increase to 8.32 Ω cm due to proton irradiation.

The Schottky barrier height evaluated for unirradiated diode is 0.53 eV. This value is close to the value of 0.58 eV reported on undoped *p*-Si-based diode [25]. Therefore, Schottky barrier height presented in this work is within the range of those reported on the reviewed literature. The Schottky barrier height evaluated from irradiated diode is 0.68 eV which is close to the value (0.66 eV) obtained in platinum-doped *p*-Si-based diode [25]. This value is higher than that of the unirradiated diode due to radiation-induced defects in the material. Additionally, the increase in Schottky barrier height is due to an increase in built-in voltage after irradiation. The built-in voltage increased from 0.3 V for unirradiated diode to 0.4 V for irradiated diode. The increase in built-in voltage after proton irradiation could be attributed to the reduction of free carrier density in the depletion region of the material through the occurrence of traps and recombination centres associated with radiation induced defects [26].

The Schottky barrier height evaluated using *C-V* technique is less than that obtained using *I-V* technique. The discrepancy may be due to the presence of interfacial layer and oxide layer at the *m-s* interface [27,28]. Also, the current in the *I-V* measurements is dominated by current that flows through the region of low Schottky barrier height while the one through *C-V* is influenced by distribution of charge at the depletion region boundary [29]. In addition, according to Refs. [30,31] the reason for this difference is attributed to inhomogeneous metal-semiconductor contact. The Schottky barrier height obtained from *C-V* is governed by

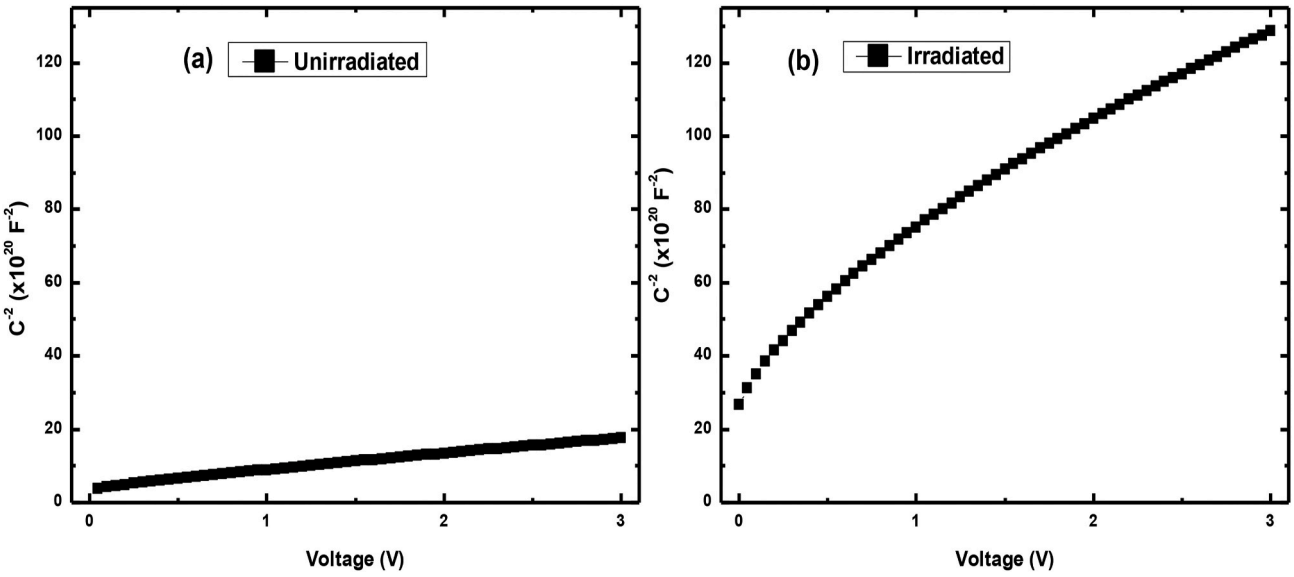

Fig. 4. C $^{-2}$-V characteristics of unirradiated (a) and proton irradiated (b) diodes.

Table 2
A summary of device parameters evaluated from C^{-2}-V plots of unirradiated and proton irradiated n-Si diodes.

Parameter	Unirradiated	Irradiated
Doping density, N_D ($\times$ 10^{15} cm^{-3})	3.36	0.53
Schottky barrier height, Φ(eV)	0.53	0.68
Built-in Voltage V_{bi}(eV)	0.30	0.40

depletion region and is less sensitive to small scale inhomogeneity unlike the one obtained from I-V [30].

4. Conclusions

A change in I-V and C-V properties of n-Si-based diodes due to 3 MeV protons was studied. A decrease in diode current and capacitance indicated that charge carrier density in the space charge region has decreased after proton irradiation. This decrease is explained in terms of radiation induced defects that are responsible for recombination of free charge carriers resulting in an increase in the resistivity of the material. The resistivity of the material was confirmed by a change in series resistance and doping density after irradiation. A change in other diodes parameters due to irradiation was also established.

The work presented here would contribute to the quest for the improved silicon radiation-hardness where a defect-engineering strategy is a promising method. Information on the effects of radiation induced defects on electrical properties of the material-based detectors is important for a study on defect-engineered silicon. The observed drastic decrease of forward current due to irradiation also instigates more studies on device-engineering where radiation detectors can be operated in forward bias for the improved radiation sensitivity.

Author statement

D. A. Oeba: student investigator, data analysis, original draft preparation. J. O. Bodunrin: editing. S. J. Moloi: supervision, conceptualization, methodology, writing- reviewing and editing.

Declaration of competing interest

The authors declare that they have no known competing financial interests or personal relationships that could have appeared to influence the work reported in this paper.

Acknowledgement

We would like to thank Prof. D. Auret and Prof. M. Diale of the University of Pretoria for the fabrication of the devices and the continued discussions on defects in solids. This work is based on the research supported wholly by the National Research Foundation of South Africa (Grant numbers: 105292 and 114800). The World Academy of Science (TWAS) is acknowledged by J. O. Bodunrin (Grant number 116113) for studentship.

References

[1] A.B. Rosenfeld, Semiconductor Detectors in Radiation Medicine: Radiotherapy and Related Applications Radiation Detectors for Medical Applications (NATO Security through Science Series), Springer, Dordrecht, 2006, pp. 111–147.
[2] S. Terzo, et al., Radiation hard silicon particle detectors for HL-LHC—RD50 status report, Nucl. Instrum. Methods Phys. Res. 845 (2017) 177–180.
[3] D. Bechevet, M. Glaser, A. Houdayer, et al., Results of irradiation tests on standard planar silicon detectors with 7–10 MeV protons, Nucl. Instrum. Methods Phys. Res. 479 (2002) 487–497.
[4] N. Barbero, J. Forneris, V. Grilj, et al., Degredation of the charge collection efficiency of an n-type Fz silicon diode subjected to MeV proton irradiation, Nucl. Instrum. Methods Phys. Res. B 348 (2015) 260–264.
[5] Y. Gurimskaya, P. Dias de Almeida, M.F. Garcia, et al., Radiation damage in p-type EPI silicon pad diodes irradiated with proton and neutrons, Nucl. Instrum. Methods Phys. Res. 958 (2020) 162221.
[6] S. Pirollo, U. Biggeri, E. Borchi, et al., Radiation damage on p-type silicon detectors, Nucl. Instrum. Methods Phys. Res. 426 (1999) 126–130.
[7] S. Seidel, A review of design considerations for the sensor matrix in semiconductor pixel detectors for tracking in particle physics, Nucl. Instrum. Methods Phys. Res. 465 (2001) 267–296.
[8] S. Karatas, A. Turut, Electrical properties of Sn/p-Si (MS) Schottky barrier diodes to be exposed 60Co γ-ray source, Nucl. Instrum. Methods Phys. Res. 566 (2006) 584–589.
[9] A. Tataroğlu, Ş. Altindal, Electrical characteristics of 60Co γ-ray irradiated MIS Schottky diodes, Nucl. Instrum. Methods Phys. Res. B 252 (2006) 257–262.
[10] P.G. Litovchenko, A.A. Groza, V.F. Lasovetsky, et al., Radiation hardness of silicon detectors based on pre-irradiated silicon, Nucl. Instrum. Methods Phys. Res. 568 (2006) 78–82.
[11] S.J. Moloi, M. McPherson, The current and capacitance response of radiation-damaged silicon PIN diodes, Physica B 404 (2009) 3922–3929.
[12] M.K. Parida, S.T. Sundari, V. Sathia Moorthy, S. Sivakumar, Current–voltage characteristics of silicon PIN diodes irradiated in KAMINI nuclear reactor, Nucl. Instrum. Methods Phys. Res. 568 (2018) 7129–7137.
[13] L. Rajan, C. Periasamy, V. Sahula, Electrical characterization of Au/ZnO thin film Schottky diode on silicon substrate, Perspectives in Science 8 (2016) 66–68.
[14] Ö.F. Yüksel, S.B. Ocak, A.B. Selçuk, High frequency characteristics of tin oxide thin films on Si, Vacuum 82 (2008) 1183–1186.

[15] Ö. Güllü, M. Çankaya, M. Biber, A. Türüt, Gamma irradiation-induced changes at the electrical characteristics of organic-based Schottky structures, J. Phys. D Appl. Phys. 41 (2008) 135103.
[16] A. Kaya, E. Marıl, Ş. Altındal, İ. Usluc, The comparative electrical characteristics of Au/n-Si (MS) diodes with and without a 2% graphene cobalt-doped Ca3Co4Ga0.001Ox interfacial layer at room temperature, Microelectron. Eng. 149 (2016) 166–171.
[17] I.M. Afandiyeva, S. Demirezen, S. Altındal, Temperature dependence of forward and reverse bias current–voltage characteristics in Al–TiW–PtSi/n-Si Schottky barrier diodes with the amorphous diffusion barrier, J. Alloys Compd. 552 (2013) 423–429.
[18] F. Yakuphanoğlu, Electrical and photovoltaic properties of cobalt doped zinc oxide nanofiber/n-silicon diode, J. Alloys Compd. 494 (2010) 451–455.
[19] H.K. Chourasiya, P.K. Kulriya, N. Panwar, S. Kumar, Analysis of the carrier conduction mechanism in 100 MeV O7+ ion irradiated Ti/n-Si Schottky barrier structures, Nucl. Instrum. Methods Phys. Res. B 443 (2019) 43–47.
[20] Ş. Altindal, İ. Dökme, M.M. Bülbül, N. Yalçm, T. Serin, The role of the interface insulator layer and interface states on the current-transport mechanism of Schottky diodes in wide temperature range, Microelectron. Eng. 83 (2006) 499–505.
[21] V.R. Reddy, N.N.K. Reddy, Current transport mechanisms in Ru/Pd/n-GaN Schottky barrier diodes and deep level defect studies, Superlattice. Microst. 52 (2012) 484–499.
[22] P.L. Hanselaer, W.H. Laflere, R.L. Van Meirhaegle, F. Cardon F, The influence of a HF and an annealing treatment on the barrier height of p- and n-type Si MIS structures, Appl. Phys. 39 (1986) 129–133.
[23] M. Msimanga, M. McPherson, Diffusion characteristics of gold in silicon and electrical properties of silicon diodes used for developing radiation-hard detectors, Mater. Sci. Eng. B 127 (2006) 47–54.
[24] I. Missoum, Y.S. Ocak, M. Benhaliliba, C.E. Benouis, A. Chakera, Microelectronic properties of organic Schottky diodes based on MgPc for solar cell applications, Synth. Met. 214 (2016) 76–81.
[25] S.J. Moloi, M. McPherson, Capacitance–voltage behaviour of Schottky diodes fabricated on p-type silicon for radiation-hard detectors, Radiat. Phys. Chem. 85 (2013) 73–82.
[26] Ö. Güllü, F. Demir, F.E. Cimilli, M. Biber, γ-Irradiation-induced changes at the electrical characteristics of Sn/p–Si Schottky contacts, Vacuum 82 (2008) 789–793.
[27] H.Ü. Tecimer, A.B. Türüt, H. Uslu, Ş. Altındal, İ. Uslu, Temperature dependent current-transport mechanism in Au/(Zn-doped) PVA/n-GaAs Schottky barrier diodes (SBDs), Sensors and Actuators A Physical 199 (2013) 194–201.
[28] Ö. Güllü, T. Kilicoglu, A.B. Türüt, Electronic properties of the metal/organic interlayer/inorganic semiconductor sandwich device, J. Phys. Chem. Solid. 71 (2010) 351–356.
[29] S.K. Tripathi, M. Sharma, Analysis of the forward and reverse bias IV and CV characteristics on Al/PVA: n-PbSe polymer nanocomposites Schottky diode, J. Appl. Phys. 111 (2012), 074513.
[30] V.G. Bozhkov, N.A. Torkhov, A.V. Shmargunov, About the determination of the Schottky barrier height with the CV method, J. Appl. Phys. 109 (2011), 073714.
[31] S. Zeyrek, Ş. Altındal, H. Yüzer, M.M. Bülbül, Current transport mechanism in Al/Si3N4/p-Si (MIS) Schottky barrier diodes at low temperatures, Appl. Surf. Sci. 252 (2006) 2999–3010.